

## Pressure Loss Characteristics of a Finned-tube Heat Exchanger in PGSFR

Dehee Kim\*, Hyungmo Kim, Sun Rock Choi

Korea Atomic Energy Research Institute, 989-111 Daedeok-daero, Yuseong-gu, Daejeon, Korea

\*Corresponding author: dehee@kaeri.re.kr

### 1. Introduction

A finned-tube sodium-to-air heat exchanger (FHX) is employed for the Active Decay Heat Removal System (ADHRS) in the Prototype Gen-IV Sodium-cooled Fast Reactor (PGSFR).

When the ADHRS operates in decay heat removal mode upon a reactor accident, the blower mounted on the intake of the FHX feeds the air into the FHX tube bundle. In the case the blower is unavailable due to failure or power loss, the ADHRS train releases the decay heat transported from the core in a passive mode.

Pressure loss in the tube bundle region accounts for more than 80% of the total pressure loss of the air flow path from the intake to the chimney exit. Pressure loss of the air flow path is linked to the heat transfer rate because the air flow rate is determined by the balance between the system pressure loss and the forced-draft (or naturally-developed) head.

Heat transfer characteristics of the FHX was tested by utilizing the SELFA facility [1]. FHXSA code developed for design and performance analysis of the FHX was validated and verified for heat transfer [1].

In this work, the pressure loss model of the FHXSA code for the FHX tube bundle region is evaluated via experimental data and computational fluid dynamics simulation results.

### 2. Methods and Results

#### 2.1 Pressure loss correlations of the FHXSA

Fin shape and tube arrangement of the FHX is illustrated in Fig. 1. In the FHXSA code, pressure loss through the finned-tube bundle is calculated by Zukauskas correlation [2] in which transverse pitch-to-diameter, longitudinal pitch-to-diameter ratios are main factors with the fin geometry.

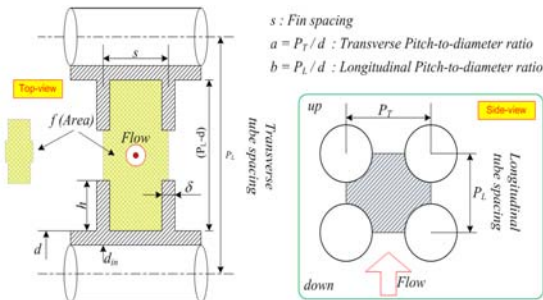


Fig. 1 Fin shape and tube arrangement of the FHX

Zukauskas correlations are given as

$$K_{drag} = 67.6 \epsilon^{0.5} Re^{-0.7} a^{-0.55} b^{-0.5} \quad (1)$$

for  $1 \times 10^2 \leq Re \leq 1 \times 10^3$ ,  
 $1.13 \leq a \leq 2.0, 1.06 \leq b \leq 2.0, 1.5 \leq \epsilon \leq 16$

$$K_{drag} = 3.2 \epsilon^{0.5} Re^{-0.25} a^{-0.55} b^{-0.5} \quad (2)$$

for  $1 \times 10^3 \leq Re \leq 1 \times 10^5$ ,  
 $1.6 \leq a \leq 4.13, 1.2 \leq b \leq 2.35, 1.9 \leq \epsilon \leq 16$

$$K_{drag} = 0.18 \epsilon^{0.5} Re^{-0.7} a^{-0.55} b^{-0.5} \quad (3)$$

for  $1 \times 10^5 \leq Re \leq 1.4 \times 10^6$ ,  
 $1.6 \leq a \leq 4.13, 1.2 \leq b \leq 2.35, 1.9 \leq \epsilon \leq 16$

Utilizing the pressure loss coefficient,  $K_{drag}$ , the pressure loss is calculated by

$$\Delta P = K_{drag} N_L c_z \left( \frac{\rho V_{max}^2}{2} \right), \quad (4)$$

where,  $V_{max}$ ,  $\epsilon$  are determined by

$$V_{max} = \frac{P_T}{P_T - d_o} V \frac{1}{R_{A,flow}}, \quad (5)$$

$$R_{A,flow} = 1 - \frac{2h\delta}{s(P_T - d_o)}, \quad (6)$$

$$\epsilon = \frac{A_{fin} + A_{tube}}{A_{tube}}, \quad (7)$$

$N_L$  is the number of tubes in the flow direction and  $c_z$  is determined by the tube configuration [2].

#### 2.2 Experiment in the SELFA facility

Model FHX (M-FHX) of the SELFA facility was designed to test the thermo-hydraulic performance test of the FHX. M-FHX has 12 tubes with same configuration of the PGSFR FHX. Heat transfer performance was already investigated [1]. In this test, only pressure loss test was carried out without considering the tube-side sodium flow. Schematic diagram is shown in Fig.2. Pressure differential through section "4" was measured for varying mass flow rates. The mass flow rates were set considering the operation conditions of the ADHRS. Section "1" has an elbow, a vertical duct, a connecting duct between the duct and the casing, a diffuser to the casing and section "3" has similar parts with the section "1", i.e., a converging nozzle, a connecting duct, a vertical duct and an elbow. Finned-tube bundles are installed in section "2".

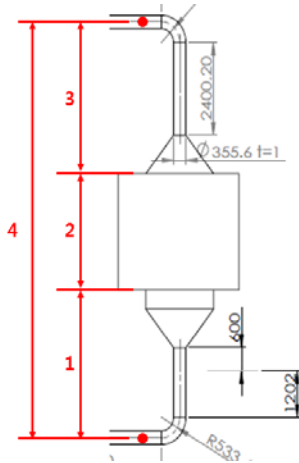


Fig. 2 SELFA facility to test the FHX

In the code, pressure loss coefficients through the flow path were implemented which are described in Diagram 6-1 for the elbows, Diagram 5-23 for the converging nozzles, Diagram 5-2 for the diffusers in the reference [3].

### 2.3 Comparison of the experimental data and the code results

The pressure loss in the section “4” (refer to Fig. 2) was measured for various mass flow rates. Mass flow rates range between 0.444 kg/s and 3.220 kg/s. These experimental data were compared with the results obtained from the FHXSA code. Fig. 3 shows the comparison results. Difference between the two data is in the range from -2% to -15% which shows appropriate implementation of the pressure loss coefficient models for the FHXSA code.

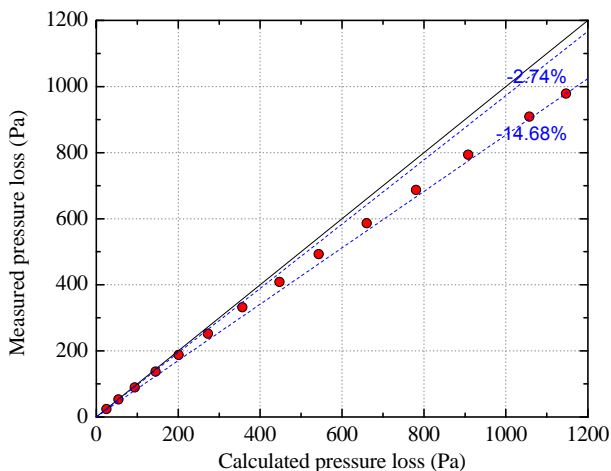


Fig. 3 Comparison of the experimental data and the code results

The FHXSA code produced more conservative results than the experimental data. Since pressure drop was measured through tube bundle region, inlet and outlet ducts, connecting parts such as converging and diverging

nozzles, CFD simulation results were utilized to estimate accuracy of the pressure loss model in the FHXSA code only for the tube bundle region.

### 2.4 Comparison of the code with the CFD simulation

Full scale CFD simulation for the PGSFR FHX was not practical because it requires too much computational resources due to the enormous grid points. Pressure loss in the tube bundle region was already calculated using STAR-CCM+ 9.02.007 in which 1/10 scaled tube in length was modelled and 3 tubes were simulated [4]. Mass flow rate and number of tubes for the scaled FHX model is 1/320 and 1/32 of the PGSFR FHX, respectively. Grid convergence test was completed and finally computational domain was filled with about 26,000,000 cells. The k- $\omega$  SST model was applied for turbulent flow analysis.

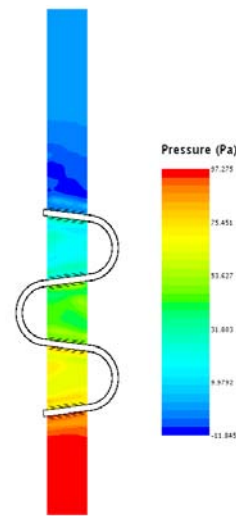


Fig. 4 Shell-side pressure distribution

Fig.4 shows the simulation result. Comparison between the CFD simulation and the code calculation is shown in Table 1. For the bundle region, the FHXSA code produces more conservative pressure loss than the CFD result. The pressure loss model implemented in the FHXSA code is best suited to compactly arranged tube bundle but the PGSFR FHX has a space between tube segments due to tube inclination angle and tube bends. These design characteristics draws disparity between the FHXSA code and the CFD results.

Table 1. Comparison between the CFD and the FHXSA

Design parameter	CFD	FHXSA	Diff(%)
Outlet temp. (°C)	252.8	259.8	2.7
Pressure loss (Pa)	94.5	143.9	34.3

### 3. Conclusions

Shell-side pressure loss correlations of the FHXSA code were evaluated through experimental and

simulation works. It is found out that the pressure loss correlations are appropriate for the conservative design of the FHX.

#### **ACKNOWLEDGEMENT**

This work was supported by the National Research Foundation of Korea (NRF) grant funded by the Korean Government (MSIP). (No. 2012M2A8A2025624)

#### **REFERENCES**

- [1] H. Kim, J. Kim, D. Kim, J. Eoh, and J.-Y. Jeong, Heat Transfer Investigation of a Cross Flow Air Heat Exchanger with Serpentine Tubes in Staggered Arrangement, KSME Summer Meeting, 2018.
- [2] A. Zukauskas, High-performance Single-phase Heat Exchangers, 3rd Edition, Hemisphere Publishing Corporation, 1989.
- [3] I. E. Idelchik, Handbook of Hydraulic Resistance, 3rd ed., Hemisphere Publishing Corporation, 1996.
- [4] S.H. Ryu, H. Ye, J. Hong, J. Yoon, D. Kim, and T. Lee, Verification of thermal-hydraulic performance of forced-draft heat exchanger in PGSFR using CFD, KSFM Summer Meeting, 2015.